



Liquid–liquid microextraction based on a dispersion of Pd nanoparticles combined with ETAAS for sensitive Hg determination in water samples

Estefanía M. Martinis^{a,b}, Leticia B. Escudero^{b,c}, Roberto Salvarezza^{b,d}, Matias F. Calderón^{b,d}, Francisco J. Ibañez^{b,d}, Rodolfo G. Wuilloud^{a,b,*}

^a Laboratory of Analytical Chemistry for Research and Development (QUIANID), Instituto de Ciencias Básicas, Universidad Nacional de Cuyo, Padre J. Contreras 1300, Parque Gral. San Martín, M5502JMA Mendoza, Argentina

^b Consejo Nacional de Investigaciones Científicas y Técnicas (CONICET), Argentina

^c Instituto de Química de San Luis, Universidad Nacional de San Luis (INQUISAL-UNSL), San Luis, Argentina

^d Instituto de Investigaciones Físicoquímicas Teóricas y Aplicadas (INIFTA), Universidad Nacional de la Plata, CONICET, La Plata, Argentina

ARTICLE INFO

Article history:

Received 19 October 2012

Received in revised form

26 February 2013

Accepted 27 February 2013

Available online 7 March 2013

Keywords:

Organic-coated Pd nanoparticles

Microextraction

Mercury

Preconcentration

ABSTRACT

A novel and highly efficient microextraction methodology based on the use of palladium nanoparticles (Pd NPs) was developed for the preconcentration and determination of Hg in water samples. Selective separation of the analyte was achieved by application of dodecanethiolate-coated Pd monolayer-protected clusters (C12S Pd MPCs) in a liquid–liquid microextraction technique (LLME). A volume of 20 μL of toluene phase containing C12S Pd MPCs was used for extraction and final phase was injected in an electrothermal atomic absorption spectrometer (ETAAS) for Hg detection. The effects of different variables, such as sample volume, extraction time, and NPs dispersion volume were carefully studied. A sensitivity enhancement factor of 95 was obtained under optimal experimental conditions. Furthermore, low detection limit (7.5 ng L^{-1}) and good precision (relative standard deviation of 4.1% at $0.25 \text{ } \mu\text{g L}^{-1}$ Hg and $n=10$) were achieved. The proposed method can be considered as a rapid, cost-effective, and efficient alternative for Hg determination in water samples like river, lake, mineral and tap water.

© 2013 Elsevier B.V. All rights reserved.

1. Introduction

Liquid–liquid extraction (LLE) has been widely used as a sample preparation technique for separation and preconcentration of organic and inorganic analytes from aqueous samples [1]. Nevertheless, this technique has several drawbacks, mainly because of the need for large volumes of solvents, making LLE an expensive and environmentally-unfriendly technique. On the other hand, miniaturized techniques [e.g., liquid–liquid microextraction (LLME)] have arisen in the search for alternatives to conventional LLE, using negligible volumes of extracting solvents and reducing the number of steps in the procedure [2]. Recent developments have led to different approaches of LLME, namely single-drop microextraction (SDME), hollow-fiber LPME (HF-LPME), dispersive liquid–liquid microextraction (DLLME) and solidified floating organic drop microextraction (SFODME) [2,3]. LLME techniques require highly efficient extractant phases.

* Corresponding author at: Laboratory of Analytical Chemistry for Research and Development (QUIANID), Instituto de Ciencias Básicas, Universidad Nacional de Cuyo, Padre J. Contreras 1300, Parque Gral. San Martín, M5502JMA Mendoza, Argentina. Tel.: +54 261 4259738.

E-mail address: rwuilloud@mendoza-conicet.gob.ar (R.G. Wuilloud).

However, conventional solvents in LLME could lead to low efficiency and time consuming extraction process. Therefore, other extractant phases are subject of recent investigation [2].

Metal nanoparticles (NPs) with a characteristic high surface to volume ratio exhibit very interesting electronic, optical, magnetic, and chemical properties, which are usually not observed with their bulk counterparts [4]. Because of their special properties, nanometer-sized materials have attracted substantial interest in the scientific community. Nanomaterials have been used in various scientific fields such as biotechnology, engineering, biomedical, environmental, and materials science [5–7]. Generally, their interesting properties lead to remarkable improvements in analytical performance [8].

The properties of NPs depend not only on their diameter, shape and size-distribution but also on their concentration, type of stabilizer in the medium, and on the nature of the interaction between metal surface and stabilizer [9]. Stabilization of metal clusters by organic coatings allows further manipulation and solubility control, which facilitates applications in different fields [10,11]. Thus, surface modification with functional groups grafted on the NPs surface prevents its agglomeration and controls the particle size during nucleation and growth in the synthesis [12,13]. Moreover, this strategy could provide extra selectivity

when NPs are used as separation media [14,15]. With the success of using chelating agents in the removal of heavy metals from aqueous solution [16,17], it seems practical to use alkanethiol-coated metal clusters as organic coordinating agents in order to accomplish similar goals for heavy metals removal from different water samples.

Mercury has long been a worrying issue due to its high neurotoxicity and widespread occurrence [18,19]. Potential health risks from low levels of Hg are a subject of intense debates. Therefore, accurate determination at trace levels in water samples is a current analytical challenge [18,20]. The affinity of Hg for sulfur-containing ligands has been well established [21,22]. Based on that observation, dodecanethiol not only could be used as stabilizer for NPs, but also, as extractant phase for Hg cations. Metal NPs have been previously used for colorimetric detection of Hg based on plasmons changes caused by Hg–metal (Au) interaction [23–25]. When NPs approach each other and aggregate, the color of NPs changes from red to purple (or blue) for Au NPs due to the shift of surface plasmon band to longer wavelength. This method is a simple and rapid approach for sensitive colorimetric detection of Hg. However, the poor selectivity observed with colorimetric-based methods limits its application in complex matrix samples. Recently, Au-coated silica NPs packed in a microcolumn have been reported for the analysis of Hg in natural waters [26]. The method was based on the preconcentration of dissolved Hg species on a catalytically active Au trap placed in a flow injection analysis system (FIAS). Thermal desorption released Hg⁰ vapor followed by atomic fluorescence spectrometry (AFS) detection. This method substantially diminished the risk of contamination, but special equipment was required. On the other hand, the combination of LLME with coordinating NPs dispersed in organic solvents could result into very attractive phases for trace element determination. To the best of our knowledge, there are no reports on NPs application in LLME systems for Hg determination.

In this work, extraction and preconcentration of Hg by dodecanethiolate-coated Pd monolayer-protected clusters (C12S Pd MPC) dispersion is proposed. A procedure involving C12S Pd MPCs and implemented using the LLME technique was developed for separation, preconcentration, and determination of Hg. The metal extracted into the organic phase was detected by direct injection into ETAAS. This methodology shows substantial improvements on various aspects as compared to earlier works

[27,28], by making possible analyte separation from water samples (i.e.; tap, mineral, river, and lake water samples) and subsequent preconcentration with a minimal amount of solvent. Thus, a green, simple, sensitive, and cost-effective method is proposed for determination of Hg at trace levels.

2. Experimental

2.1. Instrumentation

Elemental detection was performed using a PerkinElmer 5100ZL atomic absorption spectrometer (PerkinElmer, Norwalk, CT, USA) equipped with a pyrolytic graphite tube (PerkinElmer) and a transversely heated graphite atomizer Zeeman-effect background correction system. A Hg electrodeless discharge lamp (EDL; PerkinElmer) operated at a current of 170 mA (modulated operation) and a wavelength of 253.7 nm with a spectral band pass of 0.7 nm was used. All measurements were made based on absorbance signals with an integration time of 5 s. The temperature vs. time program for the atomizer is fully depicted in Table 1.

A centrifuge (Luguimac, Buenos Aires, Argentina) model LC-15 was used to accelerate the phase separation process. A vortex model Bio Vortex V1 (Boeco, Hamburg, Germany) was used for mixing the reagents. A Horiba F-51pH meter (Kyoto, Japan) was used for pH determinations.

UV–vis plots were acquired with a UV–vis PerkinElmer Lambda 35TM Spectrophotometer in a wavelength range between 300 and 900 nm. FT-IR measurements were acquired with a PIKE MiracleTM Varian 600 Instrument run in the transmission mode. Atomic force microscope (AFM) images were acquired with a Veeco Digital Instruments Nanoscope V (Santa Barbara, CA) using a Si tip operating in the tapping mode. Pd MPCs were drop-cast deposited on highly oriented pyrolytic graphite (HOPG) for measuring cross-sections between the as-deposited material and a flat substrate.

2.2. Reagents

All reagents were of analytical grade and the presence of Hg was not detected within the working range. A 1000 µg mL⁻¹ Hg²⁺ stock solution was prepared from mercury(II) chloride (Merck, Darmstadt, Germany) in 0.1 mol L⁻¹ HNO₃ (Ultrex[®] II

Table 1
Instrumental and experimental conditions for Hg determination.

<i>Instrumental conditions</i>				
Wavelength (nm)	253.7			
Spectral band width (nm)	0.7			
EDL lamp current (mA)	170			
Modifier volume (µL)	20			
Modifier amount (µg)	10 µg Pd [Pd(NO ₃) ₂]			
<i>Graphite furnace temperature program</i>				
Step	Temperature (°C)	Ramp time (s)	Hold time (s)	Argon flow rate (mL min ⁻¹)
Drying	110	1	30	250
	130	15	30	250
Pyrolysis	250	10	20	250
Atomization	1300	1	5	0
Cleaning	2400	1	2	250
<i>Extraction conditions</i>				
Sample volume	3 mL			
Pd nanoparticle dispersion volume	20 µL			
Hg ²⁺ standard solution concentration	0.25 µg L ⁻¹			
Choloroform volume	25 µL			
Extraction time	3 min			

Mallinckrodt Baker, Phillipsburg, NJ, USA). Lower concentrations were prepared by diluting the stock solution with 0.1 mol L⁻¹ HNO₃. A 1000 mg L⁻¹ palladium solution as chemical modifier was prepared from Pd(NO₃)₂·2H₂O (Fluka, Buchs, Switzerland) in 0.1% (v/v) HNO₃. A 150 mg L⁻¹ Mg(NO₃)₂ (Merck) and 2500 mg L⁻¹ NH₄H₂PO₄ (Merck) stock solutions were tested as chemical modifier. These solutions were prepared in 0.1% (v/v) HNO₃. A 2.0 mol L⁻¹ acetic acid–acetate solution (Merck) adjusted to pH 6.0 by dissolution of sodium hydroxide (Merck) was employed as buffer solution. A NaNO₃ (Merck) solution 2 mol L⁻¹ was used in order to adjust ionic strength. Ultrapure water (18 MΩ cm) was obtained from a Millipore Continental Water System (Bedford, MA, USA). For the synthesis of C12S Pd MPCs the reagents used were potassium tetrachloropalladate (II) K₂PdCl₄ (99%), sodium borohydride NaBH₄ (99%), tetrabutylammonium bromide Oct₄NBr (99%), and toluene (99.9%) Plus for HPLC. Ethanol anhydrous (99.8%) Plus for HPLC and 1-dodecanethiol C12SH (98%) were purchased from Aldrich Chemical Co. Milli-Q water (17.8 MΩ*cm) was employed for all aqueous solutions. All reactions were conducted at ambient conditions.

2.3. Synthesis of dodecanethiol-coated Pd monolayer-protected clusters (C12S Pd MPCs)

C12S Pd MPCs were synthesized according to a procedure reported previously [10,29]. Briefly, K₂PdCl₄ (0.10 g) dissolved in 20 mL of H₂O was added with stirring to Oct₄NBr (0.273 g) dissolved in 100 mL of toluene in a 250 mL round bottom flask. The toluene phase turned deep red while the PdCl₄²⁻ phase, presumably as (Oct₄N⁺)PdCl₄²⁻, was transferred into it. The solution was stirred for 15–20 min, the H₂O layer removed, and 36 μL of dodecanethiol (C12S) added, leading to a lighter orange-red color solution. The NaBH₄ reducing agent (0.18 g) dissolved in 20 mL of H₂O was immediately added at room temperature causing the solution to turn black within 30–60 s, and the reaction mixture was stirred for approximately 2 h. With the aim to remove the excess of TOABr from the toluene phase, nanopure water was added and discarded from the organic solution several times. The water layer was discarded and the toluene removed under vacuum. The product was collected on a falcon tube and centrifuged three times in absolute ethanol solution. The supernatant was removed and the precipitated product was cleaned with ethanol several times. Finally, the product was dissolved in toluene and kept at low temperature for further uses.

2.4. MPCs characterization

For spectroscopy characterization, the as-synthesized C12S Pd MPCs were drop-cast deposited on a clean glass for running FT-IR (Fig. 1) and UV-vis (Fig. 2). FT-IR samples were prepared as described; however, a thicker film was needed in order to improve the signal of the instrument. Assembled films were then further drop-cast with 3 drops from a concentrated C12S Pd MPCs solution. For AFM the as-synthesized sample was drop-cast deposited on highly oriented pyrolytic graphite (HOPG) which provided atomically smooth terraces for nanoparticles observation. The average diameter of Pd nanoparticles is ~3.0 consistent with literature [10] and based on our AFM data (Fig. 3).

2.5. Sample collection and conditioning

The manipulation and analysis of the samples were developed in a clean laboratory environment. All the materials used were previously washed with a 10% (v/v) HNO₃ solution and then with ultrapure water before drying in a clean air hood. The water

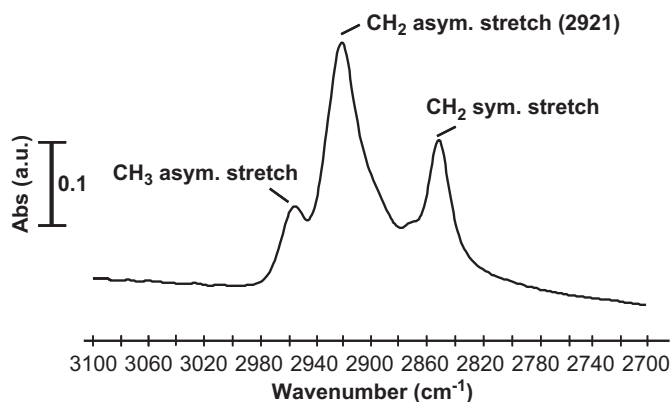


Fig. 1. FT-IR plot for as-deposited C12S Pd MPCs showing organic chain organization as indicated by CH₂ asymmetric stretch peak at 2921 cm⁻¹.

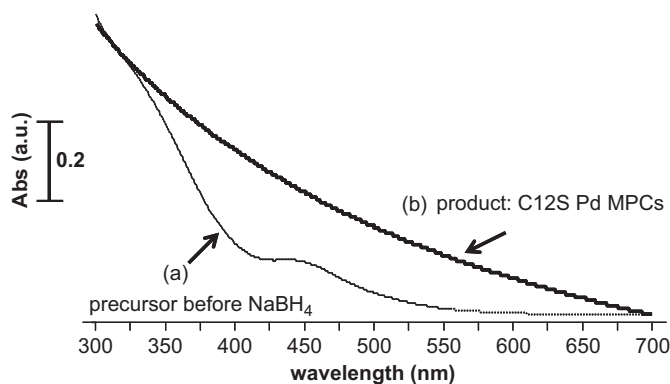


Fig. 2. UV-vis plot showing absorbance peaks for Pd(II)(TOA)₂ + Pd(II) dodecanethiolate (a) before and (b) after reduction with NaBH₄.

samples were collected in 1000 mL borosilicate glass bottles and filtered through 0.45 μm pore size membrane filters (Millipore, Bedford, MA, USA). Immediately after sampling, the 1000 mL aliquots were acidified with HNO₃ and stored at 4 °C.

2.6. Extraction and preconcentration technique

The extraction/preconcentration procedure was performed as follows: 50 μL of buffer solution 2.0 mol L⁻¹ (pH 6.0) was added to 3 mL of water sample in a centrifuge tube. For optimizing the preconcentration technique, 3 mL of 1 μg L⁻¹ Hg²⁺ standard solution was used instead of the water sample. 20 μL Pd nanoparticle dispersion in toluene mixed with 25 μL of chloroform was added to the mix and the resulting system was shaken for 3 min with a vortex. In order to separate the phases, the turbid solution was centrifuged for 7 min at 3500 rpm (1852.2g) and the aqueous phase was removed with a transfer pipette. Finally, a 20 μL aliquot of the resulting solution was analyzed by ETAAS. Instrumental and experimental conditions were as depicted in Table 1. Calibration was performed against aqueous standard solutions submitted to the same extraction procedure. Blank solutions were analyzed in the same manner as standard and sample solutions.

3. Results and discussion

To take full advantage of the procedure various experimental parameters were studied and optimized. The study of the preconcentration variables was performed by modifying one variable at a time, while keeping the others constant. This procedure allowed the study of individual effect of each variable on the

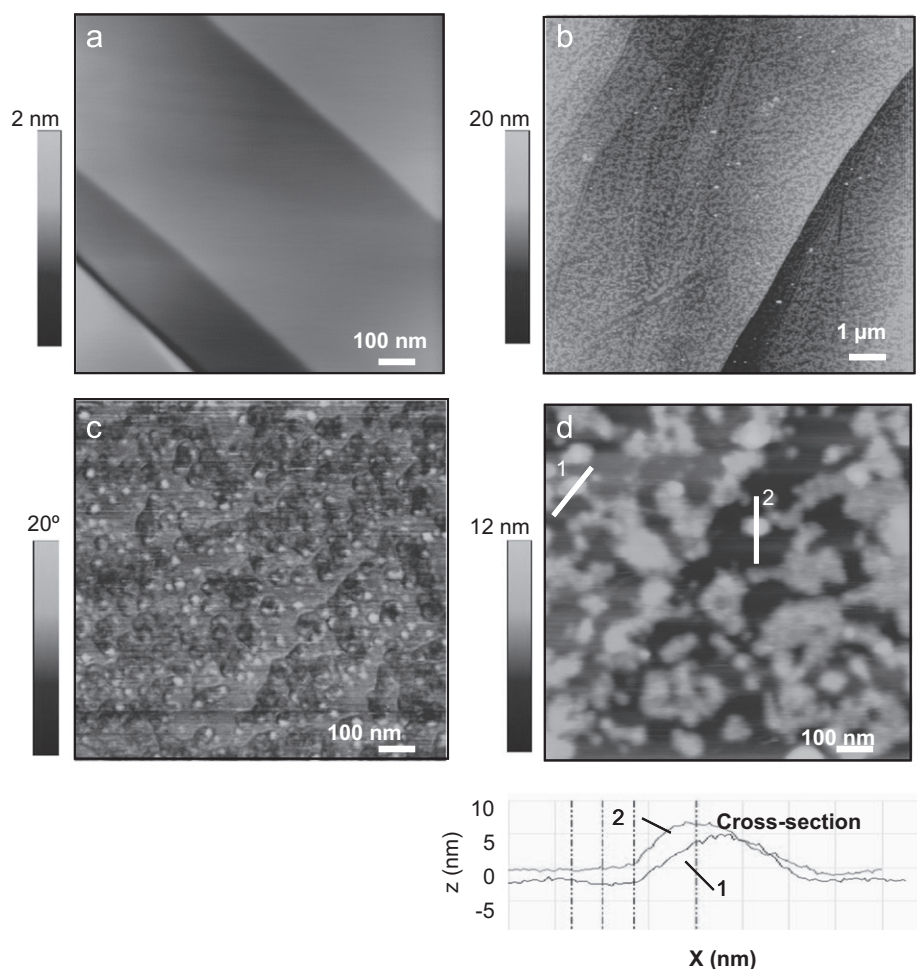


Fig. 3. AFM images of (a) bare highly oriented pyrolytic graphite (HOPG), (b) drop-cast deposited, (c) phase image, and (d) smaller image of an as-deposited C12S Pd MPCs film along with its cross-section with heights as indicated.

extraction and preconcentration of the analyte by the C12S Pd MPCs organic phase.

3.1. Evaluation of thermal treatment during ETAAS determination

Under some conditions and when analysis of trace metal in organic solvents is performed by ETAAS, favorable results may not be obtained by the same method as used for trace metal determination in an aqueous matrix. For this reason, chemical modifiers need to be added to the sample, when organic phases have to be analyzed, for preventing deterioration of sensitivity by evaporation of the target metal during the drying process. Different amounts of $\text{NH}_4\text{H}_2\text{PO}_4$, $\text{Mg}(\text{NO}_3)_2$, and $\text{Pd}(\text{NO}_3)_2$ and their mixtures were tested as chemical modifiers. The stabilization of Hg in the atomizer by Pd (10 μg) was the most effective approach. It is generally assumed that noble metals form stable amalgams with Hg [30]. In this case, Hg was retained up to 250 °C without significant losses and reduced background absorption during atomization. Therefore, 250 °C was chosen as the pyrolysis temperature. Once pyrolysis temperature was selected, the effect of atomization temperature on Hg absorption signal was studied within the range of 800–1400 °C. The maximum signal was obtained at 1300 °C. Final conditions for ETAAS detection are shown in Table 1.

3.2. Relation between pH and Hg extraction by C12S Pd MPCs

The pH value of sample solution plays a significant role in the interaction processes of analytes with the extractant phase. From

the principle of hard and soft acids and bases, Hg (a soft acid) prefers to bind with sulfur (a soft base) through covalent attachment [31]. Depending on pH, the Hg species that are likely to interact with thiol groups are Hg^{2+} , HgOH^+ , and $\text{Hg}(\text{OH})_2$. When Hg is in the form of Hg^{2+} , its complexation with thiol groups leads to the formation of a positive charge complex, which requires an anion to be neutralized. Therefore, the formation of positively charged complexes acts as an electrostatic barrier limiting the further complexation of large quantities of positively charged species such as Hg^{2+} . On the other hand, no electrostatic restrictions are expected to occur at pH above 4. Therefore, the effect of pH on Hg extraction was studied in the pH range between 4 and 11 by adding diluted HCl or NaOH solutions. As can be observed in Fig. 4, the highest extraction efficiency was achieved between pH 5 and 7. In this pH range, the reaction of hydroxylated Hg species (HgOH^+ and $\text{Hg}(\text{OH})_2$) with thiol groups resulted in the formation of a neutral complex, indicating that no electrostatic restrictions occurred. A pH value of 6 was chosen for further experiments. Acetic acid/acetate buffer was chosen as optimal according to the working pH defined previously.

3.3. Effect of C12S Pd MPCs dispersion volume, shaking and centrifugation time on the extraction efficiency

C12S Pd MPCs are hybrid materials composed of a metallic core (see UV–vis plot in Fig. 2) surrounded by organo alkanethiols with exceptionally high surface area [10,12]. Our experiments demonstrate that MPCs improved sorption properties toward Hg,

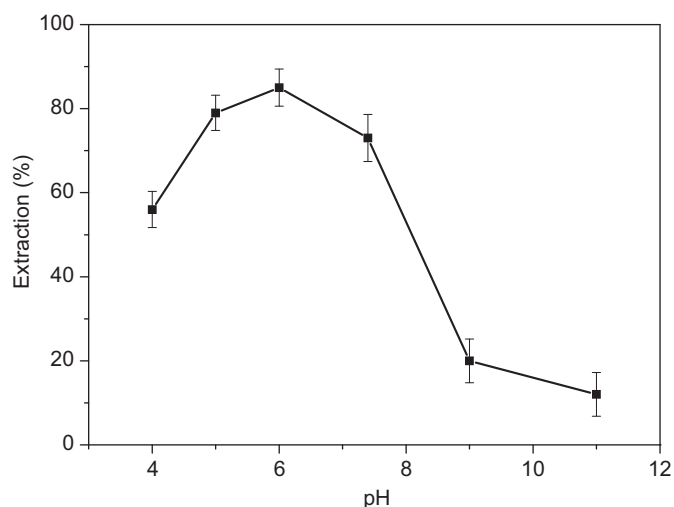


Fig. 4. Effect of pH on Hg extraction by C12S Pd MPCs. Each desired pH was obtained by adding suitable amounts of diluted HCl or NaOH. Experimental conditions are listed in Table 1.

superior by far to those achieved with just neat thiols in solution. When the extraction was performed with C12S Pd MPCs as extractant phase instead of dodecanethiol solution, an increase of 22% in extraction percentage was obtained. C12S Pd MPCs thus significantly enhanced Hg accessibility to the binding sites with respect to dodecanethiol solution of the same concentration. Therefore, higher Hg extraction by alkanethiol-coated Pd nanoparticles as compared to neat thiols can be attributable to the large surface area exposed to the analyte of interest. Fig. 3 shows an atomic force microscope (AFM) image of a film comprising C12S Pd MPCs with 3.0 nm average nanoparticle diameter. The study of monolayer-protected Au cluster in the literature [12] indicates that surface atoms dominate by 80% of the total atoms in a nanoparticle. Accordingly, for a ~ 3 nm diameter Au nanoparticle there are 390 atoms in the surface and 187 alkane chains surrounding the metal core. Therefore, the improved preconcentration of Hg observed in C12S Pd MPCs with respect to neat thiols could be consistent with high surface area provided by Pd nanoparticles and readily active sites toward the interaction between Hg and RS-Pd as well as Hg with Pd surface. It is wellknown that heavy metal ions are metallophilic [32] (attracted to Pd in this case) but they are also known to form mercaptans which involves the interaction of sulfur-containing molecules with Hg. In this regard, more experiments are underway in order to better elucidate the complex chemistry involved in these interactions. We performed FT-IR of the as-synthesized Pd MPCs just to gain insights into the organic layer by looking at the asymmetric (d^-) CH_2 stretching vibration. For instance, alkanethiols on Au usually chemisorb in a well-organized fashion caused by Van der Waals interactions between hydrocarbons. Moreover, it has been proved that the surface of nanoparticles provides order to the organic ligands as demonstrated when comparing neat thiols to thiols assembled on MPCs [33,34]. Fig. 3 shows as-deposited C12S Pd MPCs with (d^-) at $\sim 2921\text{ cm}^{-1}$ indicating alkane chain order when compared to neat dodecanethiols ($\sim 2925\text{ cm}^{-1}$) [35]. In addition, the regular structure of these materials in combination with LLME resulted in faster adsorption rates (3 min) with respect to previous reported works using mercaptants attached to different silica-like materials (2 h) [27,28].

The volume of Pd nanoparticle dispersed phase used in this preconcentration procedure was a critical factor to obtain high analytical recoveries. The effect of the extraction phase on the preconcentration of Hg was investigated in the range 10–60 μL

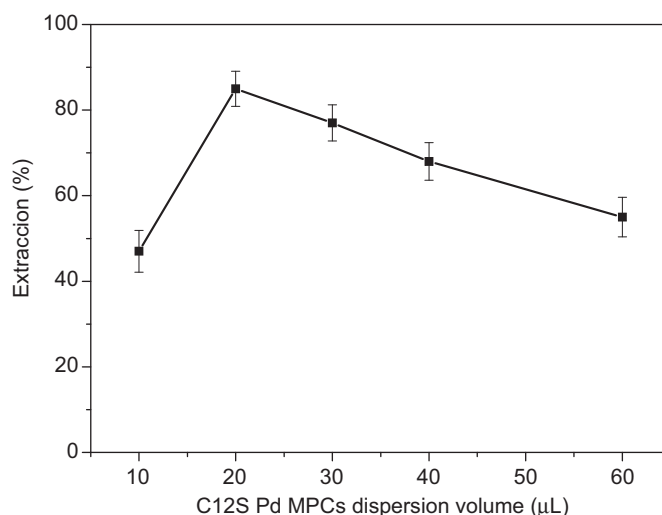


Fig. 5. Effect of C12S Pd MPCs dispersion volume on the extraction capacity of the system. Experimental conditions are listed in Table 1.

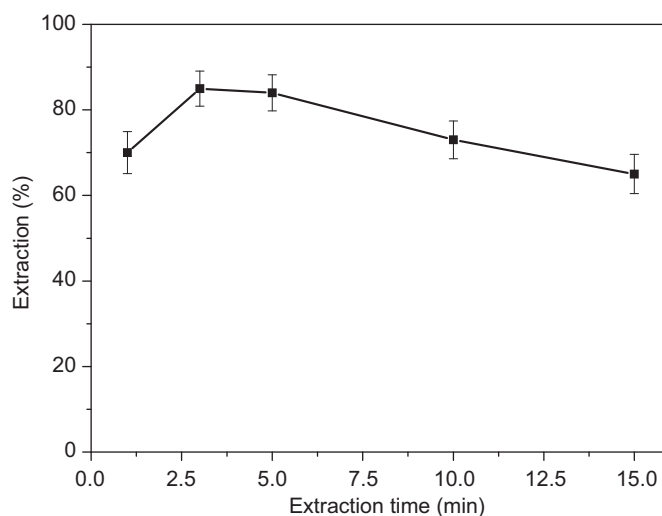


Fig. 6. Effect of the extraction time on the extraction efficiency of the system. Other conditions were as indicated in Table 1.

for a Pd concentration of 0.042 mol L^{-1} . As Fig. 5 shows, the extraction efficiency of the system increased up to 20 μL of the dispersion. Dispersion volumes smaller than 20 μL led to a reduction of the analytical response due to incomplete partitioning of the analyte while larger volumes significantly reduced the preconcentration factor. Therefore, a volume of 20 μL was used in the proposed method.

Finally, the effectiveness of Hg^{2+} extraction under the influence of shaking and centrifugation was studied in this work. A 3 min shaking time (Fig. 6) and a 7 min centrifugation time at 3500 rpm (1852.2g) were selected as optimum since complete separation occurred and no appreciable improvements on analyte extraction were observed for longer time.

3.4. Effect of sample volume on the extraction system

Sample volume was studied in order to optimize the preconcentration factor of the analytical technique. Quantitative extraction was observed for a sample volume range of 1–3 mL. Higher sample volumes partially solubilized the organic phase, leading to non-reproducible results. Therefore, a 3 mL sample volume was selected in order to obtain the higher preconcentration factor.

3.5. Effect of chloroform on the extraction system

The volume of chloroform is one of the variables determining the extraction efficiency in this technique, as it affects both surface tension of the organic phase and sedimentation of the extractant phase. Therefore, a more efficient mass transfer from aqueous solution to the organic phase can be expected when size of organic drops is diminished and hence surface area between the two phases increases. This strategy was assayed based on the fact that surface tension of the organic phase could be diminished in the presence of another solvent [36], thus improving the diffusion of Hg into the extractant phase. The effect of chloroform volume on Hg extraction was investigated in the range of 10–60 μL . Precipitation of the organic phase did not occur for volumes lower than 20 μL . For chloroform volumes larger than 35 μL , a reduction (16%) of the preconcentration factor was observed. Thus, a 25 μL chloroform volume was selected in this study.

3.6. Influence of ionic strength and potential interfering species

The extraction system was studied within an ionic strength range of 0–1 mol L^{-1} , adjusted with NaNO_3 . The ionic strength did not influence the system performance within the studied range.

Table 2

Determination of Hg in water samples and analyte recovery study (95% confidence interval; $n=6$).

Sample	Base value ($\mu\text{g L}^{-1}$)	Quantity of Hg^{2+} added ($\mu\text{g L}^{-1}$)	Quantity of Hg^{2+} found ($\mu\text{g L}^{-1}$)	Recovery (%) ^a
Mineral water	0.09	–	0.09 ± 0.01	–
	0.09	0.5	0.58 ± 0.03	98.2
	0.09	1	1.08 ± 0.05	98.9
Mineral water	0.06	–	0.06 ± 0.01	–
	0.06	0.5	0.56 ± 0.03	99.8
	0.06	1	1.02 ± 0.04	95.6
Tap water 1	0.1	–	0.10 ± 0.01	–
	0.1	0.5	0.63 ± 0.04	105
	0.1	1	1.10 ± 0.05	100
Tap water 2	0.12	–	0.12 ± 0.01	–
	0.12	0.5	0.60 ± 0.03	96.0
	0.12	1	1.14 ± 0.05	102
River water 1	0.05	–	0.05 ± 0.01	–
	0.05	0.5	0.54 ± 0.04	98.4
	0.05	1	1.06 ± 0.05	101
River water 2	< LOD	–	< LOD	–
	< LOD	0.5	0.60 ± 0.03	103
	< LOD	1	1.13 ± 0.04	105
Lake water 1	0.08	–	0.04 ± 0.01	–
	0.08	0.5	0.54 ± 0.03	99.4
	0.08	1	1.02 ± 0.05	97.5
Lake water 2	0.04	–	–	–
	0.04	0.5	0.51 ± 0.03	103
	0.04	1	1.00 ± 0.05	100

^a $100[(\text{found} - \text{base})/\text{added}]$.

The effect of concomitant ions regularly found in natural water samples was also evaluated in this work. The study was performed by analyzing 3 mL of $0.5 \mu\text{g L}^{-1}$ Hg solution containing concomitant ions at different concentrations, according to the recommended extraction procedure. A concomitant ion was considered to interfere if it resulted in an analytical signal variation of $\pm 5\%$. Thus, Cu^{2+} , Zn^{2+} , Ni^{2+} , Co^{2+} , Mn^{2+} and Fe^{3+} could be tolerated up to at least $100 \mu\text{g L}^{-1}$. Analytical signal of the blank was not modified in the presence of the concomitant ions assayed.

3.7. Analytical performance and determination of Hg in real samples

The relative standard deviation (RSD) resulting from the analysis of 10 replicates of 3 mL of a solution containing $0.25 \mu\text{g L}^{-1}$ of Hg^{2+} was 4.1%. Analytical sensitivity was enhanced by a factor of 95. This enhancement factor was obtained from the ratio of the calibration curve slopes for Hg with and without application of the extraction/preconcentration step. Calibration curve without preconcentration was obtained by directly injecting 20 μL of Hg standard solutions at different concentrations into ETAAS. The calibration graph obtained with the proposed method was linear with a correlation coefficient of 0.9997 from levels near the detection limits and up to at least $10 \mu\text{g L}^{-1}$. The limit of detection (LOD) was calculated based on the signal at intercept and three times the standard deviation about regression of the calibration curve [37]. A LOD of 7.5 ng L^{-1} Hg was obtained for the proposed methodology.

The accuracy of the proposed method was evaluated by analysis of a certified reference material (CRM), QC Metal LL3 Mercury in Water (VKI Reference Materials), with a Hg concentration of $6.48 \pm 0.51 \mu\text{g L}^{-1}$. The concentration of Hg found in this CRM after applying the proposed method was $6.41 \pm 0.15 \mu\text{g L}^{-1}$ (95% confidence interval; $n=6$). Likewise, the method was applied for Hg determination in different water samples taken from Mendoza province (Argentina). Hg concentrations in water samples were in the range of $0.06\text{--}0.09 \mu\text{g L}^{-1}$ for mineral water, $0.10\text{--}0.12 \mu\text{g L}^{-1}$ for tap water, $< \text{LOD}\text{--}0.05 \mu\text{g L}^{-1}$ for river water and $0.04\text{--}0.08 \mu\text{g L}^{-1}$ for lake water. Furthermore, a recovery study was developed on samples spiked at known concentration levels of Hg. The results are shown in Table 2. Recoveries of Hg varied between 95.6% and 105%. Finally, a comparison to other methods reported in the literature for Hg determination is given in Table 3. The proposed method requires lower volume of sample and reagents, significantly diminishing waste generation in the analytical laboratory. In addition, our method shows lower LOD, higher precision and a higher enhancement factor than those of other works already reported (Table 3). Moreover, this method can be considered as a simple and selective approach for Hg detection.

4. Conclusions

In this work, a novel and sensitive analytical methodology for Hg preconcentration and determination in different water samples using thiol-stabilized Pd nanoparticles was developed. The

Table 3

Characteristic performance data obtained by using the proposed method and others reported for Hg determination.

Method	LOD ($\mu\text{g L}^{-1}$)	RSD (%)	Enhancement factor	Sample consumption (mL)	Detection technique	Ref.
Pd-HS-SDME	0.8	8.7	72	5	ETV-ICP-MS	[38]
SPE-agar	0.02	2.6	100	250	CV-AAS	[39]
NP-Cloud point	2	6	n.r. ^a	10	UV-Vis	[40]
NP-LLME	0.0075	4.1	95	3	ETAAS	This work

^a n.r.: not reported.

use of Pd nanoparticles dispersion in biphasic systems as an alternative to conventional liquid–liquid extraction offers several advantages, including high capacity to extract Hg^{2+} without the use of external complexing reagents and its implementation in L–L microextraction. The LLME approach associated with ETAAS detection can be proposed as a low organic solvent consuming extraction technique, which turns it into a low cost and environmentally friendly tool for elemental studies. The preconcentration method allowed Hg determination in lake, river, mineral and tap water samples at trace levels (ng L^{-1}) with high accuracy and reproducibility.

Acknowledgments

This work was supported by Consejo Nacional de Investigaciones Científicas y Técnicas (CONICET), Agencia Nacional de Promoción Científica y Tecnológica (FONCYT; PICT-BID) and Universidad Nacional de Cuyo (Argentina). FJl gratefully acknowledges both PICT-PRH 295 and CONICET-NSF traveling funds (Res. 1283). RCS gratefully acknowledges ANPCyT for the PICT-2010-2554 project.

References

- [1] C. Mahugo-Santana, Z. Sosa-Ferrera, M.E. Torres-Padrón, J.J. Santana-Rodríguez, *TrAC Trends Anal. Chem.* 30 (2011) 731–748.
- [2] A. Sarafraz-Yazdi, A. Amiri, *TrAC Trends Anal. Chem.* 29 (2010) 1–14.
- [3] F. Pena-Pereira, I. Lavilla, C. Bendicho, *Spectrochim. Acta: Pt B* 64 (2009) 1–15.
- [4] R. Johnson, *Nanotechnology*, Lerner Publications Company, Minneapolis, 2006.
- [5] Y. Gao, C. He, Y. Huang, F.-L. Qing, *Polymer* 51 (2010) 5997–6004.
- [6] J. Kim, J.-H. Yun, C.-S. Han, *Curr. Appl. Phys.* 9 (2009) e38–e41.
- [7] V.V. Pokropivny, V.V. Skorokhod, *Mater. Sci. Eng.* 27 (2007) 990–993.
- [8] C.-S. Wu, F.-K. Liu, F.-H. Ko, *Anal. Bioanal. Chem.* 399 (2010) 103–118.
- [9] P. Migowski, G. Machado, S.R. Teixeira, M.C.M. Alves, J. Morais, A. Traverse, J. Dupont, *Phys. Chem. Chem. Phys.* 9 (2007) 4814–4821.
- [10] F.P. Zamborini, S.M. Gross, R.W. Murray, *Langmuir* 17 (2001) 481–488.
- [11] F.J. Ibañez, F.P. Zamborini, *Small* 8 (2012) 174–202.
- [12] M.J. Hostetler, J.E. Wingate, C.J. Zhong, J.E. Harris, R.W. Vachet, M.R. Clark, J.D. Londono, S.J. Green, J.J. Stokes, G.D. Wignall, G.L. Glush, M.D. Porter, N.D. Evans, R.W. Murray, *Langmuir* 14 (1998) 17–30.
- [13] M. Brust, M. Walker, D. Bethell, D.J. Schiffrin, R. Whyman, *J. Chem. Soc. Chem. Commun.* (1994) 801–802.
- [14] D. Sýkora, V. Kašička, I. Mikšik, P. Řezanka, K. Záruba, P. Matějka, V. Král, *J. Sep. Sci.* 33 (2010) 372–387.
- [15] Z. Zhang, B. Yan, Y. Liao, H. Liu, *Anal. Bioanal. Chem.* 391 (2008) 925–927.
- [16] H. Chen, P. Du, J. Chen, S. Hu, S. Li, H. Liu, *Talanta* 81 (2010) 176–179.
- [17] E.M. Martinis, P. Bertón, J.C. Altamirano, U. Hakala, R.G. Wuilloud, *Talanta* 80 (2010) 2034–2040.
- [18] I.A. Al-Saleh, *Int. J. Environ. Health* 3 (2009) 22–57.
- [19] A. Bhan, N.N. Sarkar, *Rev. Environ. Health* 20 (2005) 39–56.
- [20] A.S.H.G. Seiler, H. Sigel, *Handbook on Toxicity of Inorganic Compounds*, Marcel Dekker, New York, 1998.
- [21] A. Müller, E. Diemann, *Advances in Inorganic Chemistry*, Academic Press, 1987, pp. 89–122.
- [22] P. Rao, O. Enger, E. Graf, W. Hosseini, A. De Cian, J. Fischer, *Eur. J. Inorg. Chem.* 2000 (2000) 1503–1508.
- [23] D. Xu, H.W. Zhao, C.Z. Huang, L.P. Wu, W.D. Pu, J.J. Zheng, Y. Zuo, *J. Nanosci. Nanotechnol.* 12 (2012) 3006–3010.
- [24] Y. Xu, L. Deng, H. Wang, X. Ouyang, J. Zheng, J. Li, R. Yang, *Chem. Comm.* 47 (2011) 6039–6041.
- [25] X. Yang, H. Liu, J. Xu, X. Tang, H. Huang, D. Tian, *Nanotechnology* 22 (2011) 1–6.
- [26] K. Leopold, M. Foulkes, P.J. Worsfold, *Anal. Chem.* 81 (2009) 3421–3428.
- [27] C.A. Bowe, R.F. Benson, D.F. Martin, *J. Environ. Sci. Health. Part A: Toxic. Hazard. Subst. Environ. Eng.* 37 (2002) 1391–1398.
- [28] A. Walcarius, C. Delacôte, *Anal. Chim. Acta* 547 (2005) 3–13.
- [29] F.J. Ibañez, F.P. Zamborini, *Langmuir* 22 (2006) 9789–9796.
- [30] A.F. Da Silva, B. Welz, A.J. Curtius, *Spectrochim. Acta Part B* 57 (2002) 2031–2045.
- [31] T. Wajima, K. Sugawara, *Fuel Process. Technol.* 92 (2011) 1322–1327.
- [32] Y.L. Hung, T.M. Hsiung, Y.Y. Chen, Y.F. Huang, C.C. Huang, *J. Phys. Chem. C* 114 (2010) 16329–16334.
- [33] M.J. Hostetler, J.J. Stokes, R.W. Murray, *Langmuir* 12 (1996) 3604–3612.
- [34] M.C. Dalfovo, R.C. Salvarezza, F.J. Ibañez, *Anal. Chem.* 84 (2012) 4886–4892.
- [35] IR value for neat 1-dodecanethiol was obtained from the following source: (<http://webbook.nist.gov/cgi/cbook.cgi?Name=1-Dodecanethiol&Units=SI&IR=on&cUV=on#IR-Spec>).
- [36] H. Wu, T.W. Chung, *Ind. Eng. Chem. Res.* 47 (2008) 7397–7404.
- [37] J.N. Miller, J.C. Miller, *Statistics and Chemometrics for Analytical Chemistry*, Prentice Hall, New York, 2001.
- [38] S. Gil, M.T.C. de Loos-Vollebregt, C. Bendicho, *Spectrochim. Acta Part B* 64 (2009) 208–214.
- [39] N. Pourreza, K. Ghanemi, *J. Hazard. Mater.* 161 (2009) 982–987.
- [40] Z.Q. Tan, J.F. Liu, R. Liu, Y.G. Yin, G.B. Jiang, *Chem. Comm.* (2009) 7030–7032.